LAWRENCE
LIVERMORE
NATIONAL
LABORATORY

UCRL-CONF-214855

Including Long-range Interactions in Atomistic Modelling of Diffusional Phase Changes

D. R. Mason, R. E. Rudd, A. P. Sutton

August 29, 2005

17th Conference on Computer Simulation Studies in Condensed-Matter Physics
Athens, GA, United States
February 16, 2004 through February 20, 2004

Including long-range interactions in atomistic modelling of diffusional phase changes

D R Mason[1], R E Rudd[2], and A P Sutton[13]

[1] Department of Materials, Oxford University, OX1 3PH, UK
[2] Lawrence Livermore National Laboratory, 7000 East Ave., L-045, Livermore, CA 94550, USA
[3] Helsinki University of Technology, Laboratory of Computational Engineering, PO. Box 9203, FIN 02015 HUT, FINLAND.

Abstract. Phase transformations in 2xxx series aluminium alloys (Al-Cu-Mg) are investigated with an off-lattice atomistic kinetic Monte Carlo simulation incorporating the effects of strain around misfitting atoms and vacancies. Vacancy diffusion is modelled by comparing the energies of trial states, where the system is partially relaxed for each trial state. Only a limited precision is required for the energy of each trial state, determined by the value of k_BT. Since the change in the relaxation displacement field caused by a vacancy hop decays as $1/r^3$, it is sufficient to determine the next move by relaxing only those atoms in a sphere of finite radius centred on the moving vacancy. However, once the next move has been selected, the entire system is relaxed. Simulations of the early stages of phase separation in Al-Cu with elastic relaxation show an enhanced rate of clustering compared to those performed on the same system with a rigid lattice. However on a flexible lattice vacancy trapping by Mg atoms in the ternary Al-Cu-Mg system makes clustering slower than the corresponding rigid lattice calculation.

1 Introduction

The mechanical properties of commercial aluminium alloys are manipulated by the process of ageing the supersaturated solid solution. In the Al-4wt.%Cu system, copper atoms cluster together on $\{200\}_{\mathrm{Al}}$ host planes to form metastable particles known as Guinier-Preston (GP) zones. On further ageing the GP zones undergo a change of structure before transforming eventually into the thermodynamically stable θ phase $CuAl_2$, which is incoherent with the host. In the 2xxx series of alloys, magnesium is added and the precipitation sequence changes. First coherent GPB zones form as $\langle 100 \rangle$ rods, which ripen into laths of the orthorhombic S phase Al_2CuMg [1–5].

While the observed structures of GP zones are well established[6–8], and the effects of the addition of certain trace elements have been studied experimentally[9–11], modelling the effect of trace elements on kinetics is a difficult problem. Their influence may stem from the formation of complexes with vacancies, which will reduce the rate of diffusion and of phase separation. It is also possible that large trace element atoms may be attracted to small solute atoms by the concomitant reduction in strain energy of the system, and in

this way promote the formation of a co-cluster. Apart from reductions in the total strain energy of the system through such an association there may also be much shorter-range gains in bond energies. It follows that the influence of trace elements is inherently atomistic in nature, in that it stems from discrete atomic interactions with point defects such as vacancies and other solute atoms. However, misfitting atoms and vacancies interact over large distances compared with a bond length through their elastic fields. It is the requirement to treat both discrete atomic interactions and long-range elastic fields on an equal footing in dilute alloys that makes the modelling of the influence of trace elements so challenging. Our aim has been to develop a methodology to meet this challenge. Since our methodology treats atomic vacancies explicitly we are able to include the possibility that vacancies may become trapped at interfaces surrounding second-phase particles, which may lead to Brownian motion of particles as described in [12,13].

A vacancy is a centre of tensile dilation, and so it will be attracted to regions of compressive stress. The pattern of compressive stress will follow the underlying local composition of the system, enhancing the time spent by a vacancy in some areas, while reducing it in others. If the pattern of compressive stress is enhanced along particular crystallographic directions, owing to elastic anisotropy, the increased probability of finding a vacancy in these regions may be expected to influence the mobility of solute atoms there, which in turn may influence the morphology of the second-phase particle.

There are three principal steps we have taken to enable us to model diffusional processes atomistically with elastic interactions. Firstly we have improved the kinetic Monte Carlo algorithm used to select each vacancy hop, by developing an efficient combination of the stochastic first and second order residence algorithms which outperforms the n-fold way for this problem. This is described in detail elsewhere [14]. Secondly we have developed an iterative scheme based on the Lanczos method to tridiagonalise a matrix, which appears particularly suited to relaxing the system following a vacancy-atom exchange. Finally, although the relaxation propagates to the boundaries of the system, we have found that the majority of the *change* of the elastic energy due to a vacancy-atom exchange can be recovered by relaxing only those atoms in a near field region.

We demonstrate the importance of considering elastic stress effects when performing kinetic Monte Carlo simulations. We show that the harmonic lattice approximation is insufficient for accurately prediciting the difference in energy between trial Monte Carlo states. However, an approximation based on relaxing those atoms within a small sphere centred on the vacancy is enough to determine the next move, provided that eventually the whole system is relaxed after each move. Simulations of diffusion performed in the Al-Cu binary alloy system show that for a fixed number of vacancy- atom exchanges, larger clusters grow on a flexible lattice owing to the reduction in elastic strain energy this can provide. However, it is also found that since vacancies

are preferentially attracted to compressive regions, they can become trapped within emerging magnesium-rich regions in an Al-Cu-Mg ternary alloy, and this can have the opposite effect of slowing the growth rate of second-phase particles.

2 Computational method

2.1 Kinetic Monte Carlo

In our example of vacancy diffusion, adjacent atomic configurations are linked by a single vacancy-atom exchange event. Kinetic Monte Carlo[14–17] enables us to associate a meaningful time with simulated stochastic events. The probability that any one of these events will be the next to occur is proportional to the rate at which the event occurs. We have used Flynn's approximation[18] derived from dynamical theory to determine a rate for the transition based on the difference in internal energy between states. The rate of migration from state i to state j is given by

$$r_{i\to j} = \left(\frac{3}{5}\right)^{1/2} \nu_D \exp\left(-\frac{\langle c\rangle\, \Omega \Delta^2}{k_B T}\right) \exp\left(-\frac{E_j - E_i}{2k_B T}\right) \tag{1}$$

where E_i is the energy of the system in state i when the system is fully relaxed, ν_D is the Debye frequency and Ω the volume of the migrating atom. We have assumed a constant Debye frequency equal to that of pure aluminium, taken to be 1.19×10^{13} Hz. The parameter Δ is the displacement, expressed as a fraction of the bond length, at which the force on the migrating atom is a maximum, and is taken to be the constant value 0.316. $1/\langle c\rangle$ is an effective elastic compliance. For fcc crystals it is given by $1/\langle c\rangle \approx 2/15\,(3/c_{11} + 2/c_{11-c_{12}} + 1/c_{44})$. Only $1/2 < 110 >$ hops are considered. Saddle points for exchanges with the next-nearest neighbour shell of atoms are around 2eV higher in energy and so are assumed too infrequent to affect the kinetics.

We have constructed a set of relatively short-ranged Finnis-Sinclair potentials [19] for this study, described fully in [14]. They have been parameterised to reproduce elastic constants, the cohesive energy and lattice parameters of the pure metals, and we use a simple interpolation scheme for the parameters of the potentials for interactions between dissimilar atoms.

2.2 Lanczos Method for relaxation

An efficient algorithm for finding relaxed states is required because there may be many millions of configurations generated during a kinetic Monte Carlo simulation of the early stages of diffusional phase separation by a vacancy mechanism. Consider first the harmonic lattice approximation. The energy may be expanded as a Taylor series about the current configuration which

may be represented by a vector $\mathbf{x}_0$ describing the positions of each of the N atoms in the system:

$$E(\mathbf{x}_0 + \mathbf{u}) = E(\mathbf{x}_0) + \left.\frac{\partial E}{\partial \mathbf{x}}\right|_{\mathbf{x}_0} \cdot \mathbf{u} + \frac{1}{2}\mathbf{u} \cdot \left.\frac{\partial^2 E}{\partial \mathbf{x}\partial \mathbf{x}}\right|_{\mathbf{x}_0} \mathbf{u} \tag{2}$$

The vector $\mathbf{u}$ is a displacement from the current configuration $\mathbf{x}_0$, which is assumed to be small in magnitude. We identify the first derivative of the energy as (minus) the $3N$ dimensional force $\mathbf{f} = -\left.\partial E/\partial \mathbf{x}\right|_{\mathbf{x}_0}$ and the second as the matrix of force constants $\mathbf{D} = \left.\partial^2 E/\partial \mathbf{x}\partial \mathbf{x}\right|_{\mathbf{x}_0}$. These two derivatives are evaluated analytically at the current configuration $\mathbf{x}_0$ using the interatomic potentials.

Equation (2) has a minimum with respect to $\mathbf{u}$ given by

$$\mathbf{u} = \mathbf{D}^{-1}\mathbf{f} \tag{3}$$

The change in energy brought about by making this displacement from the current configuration is obtained by substituting (3) into (2), giving $\Delta E = -\frac{1}{2}\mathbf{f} \cdot \mathbf{D}^{-1}\mathbf{f}$.

For the aluminium-copper alloys of interest to this study the displacements of atoms near a vacancy are relatively large and sensitive to the local atomic structure. We have found the difference in energy between harmonically relaxed states to be in error, compared to fully relaxed states, by the order of 0.1eV. Since this is the same order as the total energy difference between states, counting both chemical bond energy changes and elastic energy changes, the harmonic relaxation approximation is seen to be unsuitable for this study.

To implement an anharmonic relaxation we have found that significant computational gains may be made if an algorithm derived from the Lanczos method of tridiagonalizing a matrix [20] is employed. The strategy is to find an approximate solution to (3) and displace atoms through this vector. The force and force constant matrix elements are then recalculated and further displacements constructed until the system energy has converged to an acceptable tolerance. Restarting the calculation in this way not only prevents error accumulation, allowing a machine precision solution if desired, but also side-steps the known problems associated with keeping the Lanczos basis vectors orthonormal.

The Lanczos method is perhaps most familiar in solid state physics in the context of calculating local densities of electronic or vibrational states [21]. Our use of the method here is quite different, namely we are generating an approximate solution for $\mathbf{u}$ in (3) for which ΔE has converged. The method constructs a new orthonormal basis set of vectors. After m such basis vectors have been generated, the subspace they span is known as the Krylov subspace: $\mathcal{K}_m(\mathbf{D}, \mathbf{f}) = \{\mathbf{f}, \mathbf{D}\mathbf{f}, \ldots, \mathbf{D}^{m-1}\mathbf{f}\}$.

The representation of $\mathbf{D}$ in this basis is the tridiagonal $m \times m$ matrix $\mathbf{T}_m$.

$$\text{define} \quad \mathbf{T}_m : \mathbf{T}_m \equiv \mathbf{\Phi}_m^T \mathbf{D} \mathbf{\Phi}_m = \begin{pmatrix} \alpha_0 & \beta_1 & & & \\ \beta_1 & \alpha_1 & \beta_2 & & \\ & \beta_2 & \alpha_2 & \ddots & \\ & & \ddots & \ddots & \beta_{m-1} \\ & & & \beta_{m-1} & \alpha_{m-1} \end{pmatrix} \tag{4}$$

where the columns of the $3N \times m$ matrix $\mathbf{\Phi}_m$ are the m generated basis vectors $\{\phi_0, \phi_1, \ldots, \phi_{m-1}\}$ each of dimension $3N$. This matrix spans the same subspace as $\mathcal{K}_m(\mathbf{D}, \mathbf{f})$.

The coefficients α and β and the basis vectors ϕ are found by the Lanczos algorithm, which is an iterative process (see e.g [20]) requiring only matrix-vector multiplies:

$$\begin{aligned} \phi_{-1} &= \mathbf{0} \ , \ \phi_0 = \frac{1}{|\mathbf{f}|}\mathbf{f} \\ \beta_{m+1}\phi_{m+1} &= \mathbf{D}\phi_m - \alpha_m\phi_m - \beta_m\phi_{m-1} \\ \text{where} \quad \alpha_m &= \phi_m \cdot \mathbf{D}\phi_m \\ \text{and} \quad \beta_m &= \begin{cases} \phi_{m-1} \cdot \mathbf{D}\phi_m & , m > 0 \\ |\mathbf{f}| & , m = 0 \end{cases} \end{aligned} \tag{5}$$

We may obtain approximate solutions for ΔE and $\mathbf{u}$ in the subspace $\mathcal{K}_m(\mathbf{D}, \mathbf{f})$. The predicted relaxation energy at this stage is

$$\Delta E_m = -{}^1\!/_2 \, |\mathbf{f}|^2 \left[\mathbf{T}_m^{-1}\right]_{00} \tag{6}$$

$\left[\mathbf{T}_m^{-1}\right]_{00}$ is the element in the top left hand-corner of the inverse of the matrix $\mathbf{T}_m$. The predicted displacement at this level is $\mathbf{u}_m = |\mathbf{f}| \, \mathbf{\Phi}_m \mathbf{T}_m^{-1} \mathbf{e}_0$, where $\mathbf{e}_0$ is the m-dimensional unit vector $[1, 0, 0, ...0]^T$. The iterative procedure of (5) can be halted when ΔE_m has converged, and then the displacement vector may be found.

We note that the displacement vector may be constructed directly from (5) as the basis vectors are constructed, in a manner analogous to that used by the method of Conjugate Gradients. However, we use an alternative method for calculating the displacement vector which is an iterative scheme using the change in energy at level m. Our method does require storing the basis vector set $\mathbf{\Phi}_m$, but we believe this extra cost to be offset by the improvement in convergence available by the method of section 2.3. We expand the displacement in the m generated basis vectors: $\mathbf{u}_m = \sum_{j=0}^{m-1} \gamma_j \phi_j$. The orthonormality condition of the basis vectors ϕ_m and (5) gives

$$\gamma_0 = -\frac{2\Delta E_m}{\beta_0} \quad , \quad \gamma_1 = \frac{\beta_0 - \gamma_0 \alpha_0}{\beta_1}$$

$$\gamma_k = -\frac{\gamma_{k-2}\beta_{k-1} + \gamma_{k-1}\alpha_{k-1}}{\beta_k} \tag{7}$$

As seen in (5), the initial vector ϕ_0 is a unit vector in $3N$ dimensional space in the direction of the force $\mathbf{f}$. Each successive multiplication by $\mathbf{D}$ in (5) enables the relaxation to spread further from the centres where the forces in $\mathbf{f}$ are located. Since the change in the relaxation energy associated with a vacancy hop decays rapidly with distance from the vacancy, a rapidly convergent estimate of the relaxation energy may be obtained, together with a good approximation to $\mathbf{u}$. Thus there is a sound physical basis for our choice of the Lanczos method to relax the system for each trial vacancy-atom exchange.

2.3 Improving the solution

We have found that the efficiency of the convergence of the Lanczos procedure can be improved by storing and reusing information generated during previous relaxations. The values of α and β found during the tridiagonalisation process can improve the estimate of the energy change after only m levels have been performed. By substituting this improved energy into (7) to (**??**), the displacement vector is also improved.

The change in energy after m levels can be written as a continued fraction (see e.g. Heine in [21]). From (6) we write

$$\Delta E_m = \cfrac{-{}^1\!/_2\beta_0^2}{\alpha_0 - \cfrac{\beta_1^2}{\alpha_1 - \cfrac{\beta_2^2}{\vdots \cfrac{}{\alpha_{m-1} - \beta_m^2}}}} \tag{8}$$

Going to another level $m+1$ does not affect the previously found coefficients α and β, but can improve the energy estimate by adding to the end of the continued fraction. It would be possible to improve the estimate of the energy change if we could terminate the continued fraction at level m with something which better represents the tail of the fraction. It is found numerically that averages a and b constructed from the coefficients α and β converge to constant values, but that even after thousands of levels the values for α and β rapidly oscillate about these averages. As a first choice, a quadratic terminator constructed from the averages could be used to replace the tail of the continued fraction at level m, by substituting β_m^2 in (8) with β_m^2/t, where:

$$a = \frac{1}{m}\sum_{j=0}^{m-1}\alpha_j, \quad b = \frac{1}{m}\sum_{j=1}^{m}\beta_j, \quad t = a - \frac{b^2}{t} = \frac{a}{2}\left(1 + \sqrt{1 - \left(\frac{2b}{a}\right)^2}\right) \tag{9}$$

The form for the quadratic terminator in (9) is valid because the discriminator is always positive.

While it is possible to ensure convergence in these averages by going to enough levels, we are looking for a displacement vector estimated from only the first few basis vectors. Too many levels of the procedure gives a well-converged solution only to the harmonic problem of (3). We find ΔE_m has typically converged to 0.1% when $\mathbf{T}_m$ is constructed to level m= 6 to 12. Note that the numerical errors at this level remain small. This is why we have no need for renormalisation of the basis set $\mathbf{\Phi}_m$. We are trying to find a displacement vector which will minimise the system energy on a weakly anharmonic potential energy surface. To converge to the true minimum we calculate the force and matrix elements at the current atom displacement, call the Lanczos procedure of 5 to generate a better solution and move the atoms. Starting from an initial position $\mathbf{x}_0$, this produces a succession of estimates for the local energy minimum $\mathbf{x}_0, \mathbf{x}_0 + \tilde{\mathbf{u}}^{(0)}, \mathbf{x}_0 + \tilde{\mathbf{u}}^{(0)} + \tilde{\mathbf{u}}^{(1)}, \ldots$, where ( ) denotes an approximated value. The displacement vectors are generated by:

$$\begin{aligned} \mathbf{D}|_{\mathbf{x}_0}\, \tilde{\mathbf{u}}^{(0)} &\approx \mathbf{f}|_{\mathbf{x}_0} \\ \mathbf{D}|_{\mathbf{x}_0+\tilde{\mathbf{u}}^{(0)}}\, \tilde{\mathbf{u}}^{(1)} &\approx \mathbf{f}|_{\mathbf{x}_0+\tilde{\mathbf{u}}^{(0)}} \\ &\ldots \end{aligned} \tag{10}$$

We are using the Newton-Raphson method to approach the solution, so the input forces $\mathbf{f}|_{\mathbf{x}_0}, \mathbf{f}|_{\mathbf{x}_0+\tilde{\mathbf{u}}^{(0)}}, \ldots$ diminish in magnitude quadratically. However, the input matrices $\mathbf{D}|_{\mathbf{x}_0}, \mathbf{D}|_{\mathbf{x}_0+\tilde{\mathbf{u}}^{(0)}}, \ldots$ change only slightly as the the position of the atoms is updated, reflecting the weakly anharmonic nature of the potentials near the minimum position.

As a function of the number of levels m, information about the extreme eigenvalues converges faster than information about the eigenvalues in the middle of the spectrum.[21] Therefore, it is possible to estimate the limits of the eigenvalue spectrum from a finite number of values of α and β. Long-range elastic interactions are determined by the properties of the lower limit of the spectrum. The short-range displacement field around a vacancy is determined primarily by the first few levels of the continued fraction. By attaching a terminator to the continued fraction not only are we able to describe long-range elastic interactions but we also embed a finite cluster centred on the vacancy in an infinite medium characterised by average elastic properties. This embedding also influences the short-range displacement field around the vacancy.

The values of the coefficients α and β to level m' are stored, and they are over-written by new values as they are generated until the criterion for convergence of the relaxation energy is satisfied. Subsequently we wish to calculate the change in the relaxation energy when a vacancy is exchanged with a neighbour. Convergence of the change in the elastic relaxation energy is attained with a smaller number, m, of exact levels. To calculate the change in the elastic relaxation we use the following continued fraction, where we

note that the first m pairs of coefficients α and β are those computed for the displaced vacancy, the remaining $m' - m$ pairs of coefficients α and β are those stored and not over-written, and t is the terminator of (9), averaged over all m' coefficients:

$$\Delta\tilde{E}_m = \cfrac{-{}^1\!/_2\beta_0^2}{\alpha_0 - \cfrac{\beta_1^2}{\vdots \cfrac{}{\alpha_{m-1} - \cfrac{\beta_m^2}{\alpha_m - \cfrac{\beta_{m+1}^2}{\vdots \cfrac{}{\alpha_{m'-1} - \cfrac{\beta_{m'}^2}{t}}}}}}} \tag{11}$$

The improved estimate for the energy change calculated using 11 is substituted in (7) to get an improved estimate for the displacement vector. Note that since the values of α and β are exact to level m, the projection of this new estimate on the true solution to (3) is greater than that available previously, even though it is within the same Krylov subspace $\mathcal{K}_m(\mathbf{D}, \mathbf{f})$.

This algorithm can be efficiently coded in parallel. A domain decomposition is used to construct the elements of $\mathbf{D}$. The matrix elements do not then need to be broadcast to perform the matrix-vector multiply in (5).

2.4 Short-range relaxation region

The displacement field around a point defect scales in magnitude as $1/r^2$, where r is the distance from the defect. Starting from a fully relaxed system of atoms, a single atom-vacancy exchange is performed to construct a new trial configuration. The additional displacement field introduced by this exchange will be dipolar, and so scale as $1/r^3$. This displacement is short-ranged and so the greatest contribution to the elastic energy change due to an exchange will come from the minor corrections of the positions of the atoms close to the exchange event.

As we are undertaking a Monte Carlo simulation, it is necessary that the energies be accurate only to within a fraction of the thermal energy. At 300K, this energy is 0.025eV. We need an approximation method which can reliably make estimates of the energy difference between states to within about 1meV.

A good approximation to the elastic energy change is found by pinning all atoms more than a fixed radius R distant from the original vacancy location, and only relaxing those within. If this is done, after relaxation only those atoms immediately exterior to the sphere will still have a finite net force acting on them. The error in the elastic energy will be due to the failure of the embedding external medium to respond to the change in shape of the

interior and vice-versa. This energy error will be positive, and scale as $1/R^3$. However, if a second virtual state is considered, it too will have an error of roughly the same size. All virtual states will therefore have a systematic component to the error due to the non-propagation of the force dipole to infinite range. An additional error component will be due to the coupling of the inhomogeneities in the far field and the force dipole. As larger near field regions are assumed, this error component will tend to zero. As this error must be kept small compared to the thermal energy, we have determined our cut-off range R to be three times the range of the potential, covering a sphere of 754 lattice sites plus the original vacancy position.

The systematic error component may be removed without affecting the statistical likelihood of selecting a given state. This error will appear in the free energy as a constant additional term, and so in the rate as a constant multiplier. If after the move the system is allowed to relax fully, then a comparison may be made between exact and approximate energies. This difference can be ascribed to the systematic error, and so the rates may be corrected. If the system is relaxed after every move, the energy of the previously visited configuration will always be stored exactly, so that the rates may be corrected even before the exchange is made.

The difference in energy between elastically relaxed states made using the short-range approximation is shown in figure 1. It can be seen that if a sufficiently large relaxation region is chosen the magnitude of the energy error can indeed be made sufficiently small. Note that our relaxation region is larger than that used previously [22–24], and that we can achieve very small errors in the energy difference by ensuring that the whole system is relaxed before each move is performed. We have chosen to use a relaxation region of 754 atoms about the original vacancy location, which produces errors in the energy of the order of 1meV.

3 Clustering in the Al-Cu and Al-Cu-Mg systems

The alloy compositions we have studied are listed in table 1. We have chosen a supercell of 10976 atoms ($14 \times 14 \times 14$ fcc unit cells) run for at least one hundred thousand vacancy exchanges. The traces for the flexible lattice calculations each took about one month of computation on four Sun UltraSPARC III 900MHx Processors. For this reason these simulations were done once only. We have modelled natural ageing, that is to say ageing at room temperature (300K) as opposed to artificial ageing at elevated temperatures. This is to provide a large driving force for clustering. We have also chosen to use a single vacancy in these diffusion simulations.

3.1 Effect of elastic strain on vacancy diffusion

Only one type of transition, a nearest neighbour vacancy-atom exchange, is permitted in this simulation. The time taken for the same number of va-

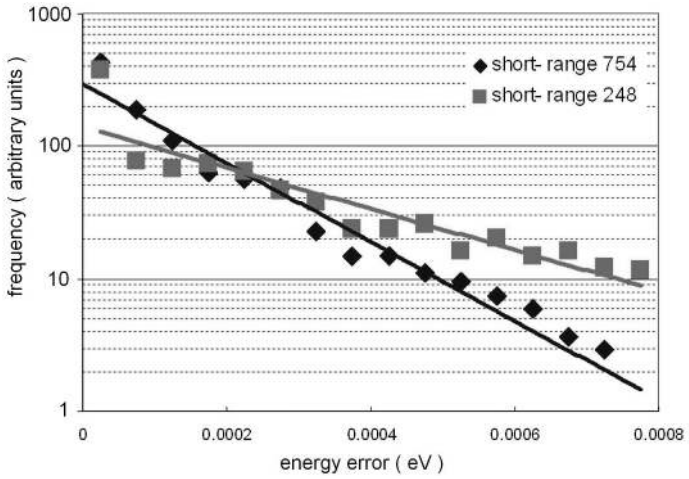

Fig. 1. Errors introduced using the short-range relaxation region, with cut-off regions encapsulating 248 and 754 atom sites centred on the original vacancy position. The vertical axis shows the frequency of errors. It is seen that the probability of the difference in energy between relaxed states being in error by more than 0.001eV becomes very small with the larger cut-off region

Table 1. Aluminium alloy compositions

alloy	aluminium			copper			magnesium		
	at.%	(wt.%)	n_{Al}	at.%	(wt.%)	n_{Cu}	at.%	(wt.%)	n_{Mg}
1	98	(95.4)	10755	2	(4.6)	220			
2	97.8	(95.2)	10733	2	(4.6)	220	0.2	(0.2)	22
3	97.5	(95.0)	10700	2	(4.6)	220	0.5	(0.4)	55
4	96	(91.1)	10536	4	(8.9)	439			
5	95.8	(90.9)	10514	4	(8.9)	439	0.2	(0.2)	22
6	95.5	(90.6)	10481	4	(8.9)	439	0.5	(0.4)	55
7.	94.0	(86.9)	10316	6	(13.1)	659			

cancy moves with and without atomic relaxation is shown in figure 2. In the case of the Al-Cu alloys, we find that running the simulation on a flexible lattice increases the real time taken for a given number of exchanges. On a flexible lattice, the real time simulated is roughly 10%-20% greater over 100000 exchanges, reflecting a commensurate decrease in the mean vacancy hopping rate. In more familiar terms the *mobility* of the vacancy is reduced on a flexible lattice. The origin of this reduction must be that the relaxations in a flexible lattice produce a greater variability in the configurational energy of the system as the vacancy migrates. In a flexible lattice the vacancy is attracted to certain sites, where it spends longer periods of time.

In the case of Al-Cu-Mg alloys, the time differences in the flexible and rigid lattices are even more pronounced, with the time simulated being 5

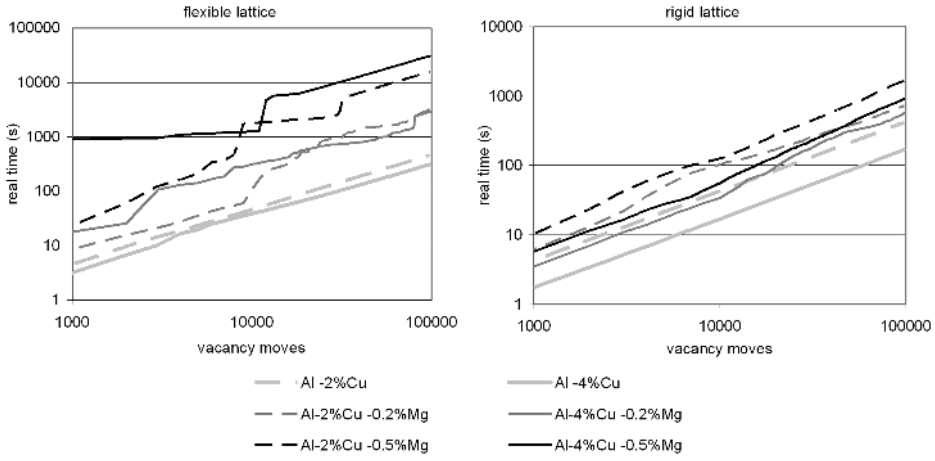

Fig. 2. Effect of performing the simulation on a flexible lattice on the real time simulated. Times shown are the simulated real time (in seconds) for a sequence of 100000 vacancy moves

times greater with 0.2% Mg (alloys 2,5), and around 10 times greater with 0.5% Mg (alloys 3,6). Note that steep steps in the plot are seen in the flexible lattice calculation when Mg is present, indicating that the vacancy is trapped temporarily. In the rigid lattice calculation these steps are absent in these early stages, although steps do appear later when there is significant clustering [14].

3.2 Effect of elastic strain on clustering

Al-Cu We now consider the short-range ordering of copper atoms. We know from separate Monte Carlo simulations using the same potentials that $L1_0$ and $L1_2$ type intermetallic structures, rather than the θ phase, are preferentially generated. There are n_{Cu} copper atoms in the system. At any time, there will be a certain number of pairs of copper atoms into pairs separated by a $< 100 >$ vector, $n_{<100>}$. Our short-range order parameter, sro_{Cu}, measures how close we are getting to this low energy intermetallic phase Al_3Cu, with structure $L1_2$: $sro_{Cu} = n_{<100>} / \left(\frac{1}{2} \times 6 \times n_{\mathrm{cu}}\right)$

We can investigate how the clustering is affected by the lattice being flexible by plotting this short-range order parameter as a function of the real time simulated. In figure 3 we plot the evolution of the short- range ordering of copper atoms in Al-Cu on a flexible and on a rigid lattice. The traces corresponding to the rigid lattice calculations are much less computationally expensive than those on a flexible lattice, and so have been generated by averaging over five independent simulation runs. The order parameter is found as the average over fixed time intervals, evenly spaced on the logarithmic real time scale.

It is clear that at all three alloy compositions simulated there is a marked *increase* in the rate of ordering of copper atoms on a flexible lattice, despite the reduction of the vacancy mobility seen in figure 2. The speed of diffusing copper atoms is determined by the product of the vacancy mobility and the force driving their motion. Therefore there must be an additional driving force for clustering on a flexible lattice as compared with a rigid lattice. Once clustering has initiated somewhere in the system it will bias the motion of other copper atoms towards the cluster along lobes of compressive stress surrounding the cluster. The additional driving force must more than compensate the reduction of the vacancy mobility to produce the increased rate of ordering of copper atoms on a flexible lattice.

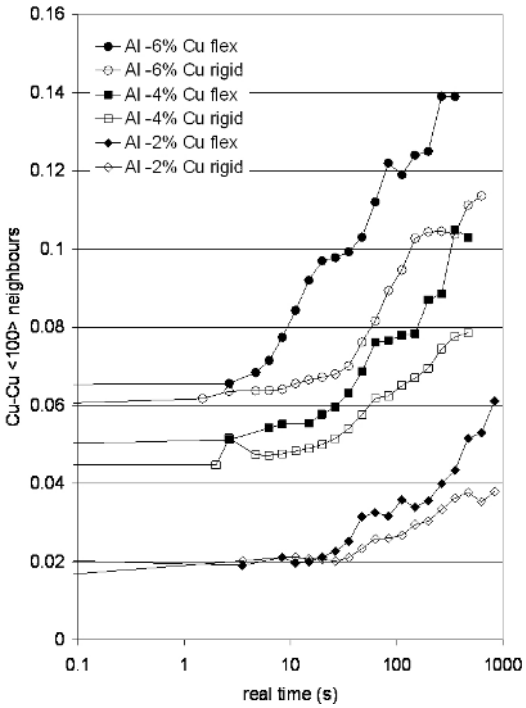

Fig. 3. Ordering in the Al-Cu system. These simulations were performed with a single vacancy in a periodic supercell of 10976 lattice points, with zero external stress, at a simulated temperature of 300K. The simulations comprised approximately 200,000 vacancy moves for alloys 1 and 7 and 250,000 moves for alloy 4. The order parameter is defined in the text. The lines are to guide the eye

Al-Cu + 0.2 at.% Mg Copper atoms are expected to be centres of tension, and magnesium atoms centres of compression in an aluminium matrix.

Therefore, there will be an attractive elastic interaction between Cu and Mg atoms on a flexible Al lattice. We might therefore expect to see Cu atoms segregating to Mg rich regions. However, the rate at which such a process occurs may be reduced by vacancies becoming trapped by Mg atoms. This trapping may be expected to occur more effectively on a flexible lattice where the motion of vacancies is biased by the elastic fields of Mg atoms, and more stable vacancy-Mg atom complexes may form through elastic relaxation.

In figure 4 we examine the effect of adding microalloying quantities of Mg atoms to Al-Cu alloys on the clustering of Cu and Mg atoms. The degree of clustering of magnesium atoms may be followed by defining an order parameter for the evolution of close packed clusters of magnesium atoms: $sro_{Mg} = n_{<1/2\,1/2\,0>} / \left(1/2 \times 12 \times n_{\mathrm{Mg}}\right)$ where $n_{<1/2\,1/2\,0>}$ is the number of $(\mathrm{Mg} - \mathrm{Mg})_{<1/2\,1/2\,0>}$ pairs, and n_{Mg} is the number of magnesium atoms present in the system. It can be seen that the rate of ordering of copper atoms is still enhanced on a flexible lattice in the presence of 0.2 at.% Mg. But, the rate of clustering of magnesium atoms is reduced on a flexible lattice until later times.

Al-Cu + 0.5 at.% Mg In figure 5 the effect of adding a higher concentration of Mg is simulated. With the higher Mg content it is no longer the case that the rate of ordering of copper atoms on a flexible lattice is enhanced.

It is seen that again the Mg atoms are clustering at a later time when the simulation is run with a flexible lattice. However, when it occurs the degree of clustering of Mg is enhanced at this higher Mg concentration.

3.3 Association of vacancies with Mg atoms

The number of magnesium atoms surrounding each vacancy is plotted as a function of time for rigid and flexible lattices in figure 6. On a rigid lattice we see that the number of magnesium atoms around a vacancy increases with time, but that this is not the case on a flexible lattice, at least for real times of up to 1000s. On the rigid lattice, magnesium clusters are forming, and the vacancies are associated with these clusters.

4 Conclusions

We have presented a method to rapidly evaluate transition rates for possible vacancy moves incorporating atomistic elastic relaxation, by approximating the saddle points as a function of the internal energy of the initial and final states. We found that the harmonic lattice approximation was insufficient for measuring the tiny difference in the elastic relaxation energy between possible vacancy moves. However a scheme based on relaxing only the local region around the vacancy was capable of reducing errors in the system energy

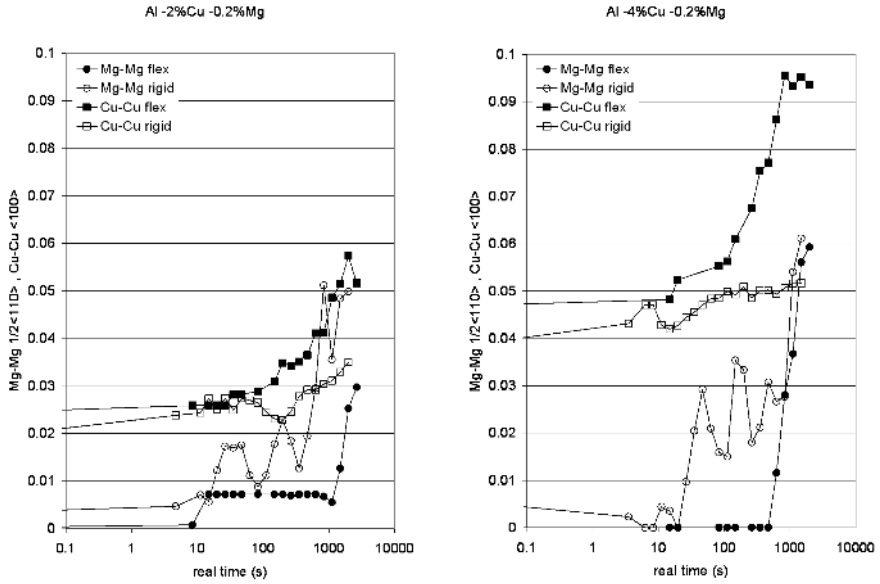

Fig. 4. Ordering in the Al-Cu-0.2%Mg system. These simulations used the same parameters as those in figure 3, and the traces were generated in the same way. The degree of clustering of Mg atoms is measured by the short range order parameter defined in (**??**). We see that there is some clustering of Mg atoms, and ordering of Cu atoms, present on both rigid and flexible lattices. The rate of ordering of copper atoms is significantly increased on the flexible lattices. The clustering of magnesium atoms seems to occur at later times on a flexible lattice as compared with a rigid lattice

to an acceptable fraction of the thermal energy. This short-range scheme was found to be successful for evaluating the transition energies for possible vacancy moves, although a full atomistic relaxation was required after the move was decided.

The Lanczos method is particularly suitable for atomic relaxation after a single vacancy move, as each iteration effectively spreads the relaxation region further from the atoms experiencing a force around the vacancy. Although the relaxations remain time- consuming, our use of this relaxation scheme has enabled us to model hundreds of thousands of vacancy moves while keeping the system atomistically relaxed.

The rate at which phase separation can occur in alloys is proportional to the mobility of vacancies and to the driving force for diffusion. Both of these may be affected by performing the simulation on a rigid lattice rather than on a flexible lattice. We have seen in figure 2 that the vacancy mobility is quite different on flexible and rigid lattices. Vacancies may be attracted to impurities through long-range elastic fields, and may form complexes that are

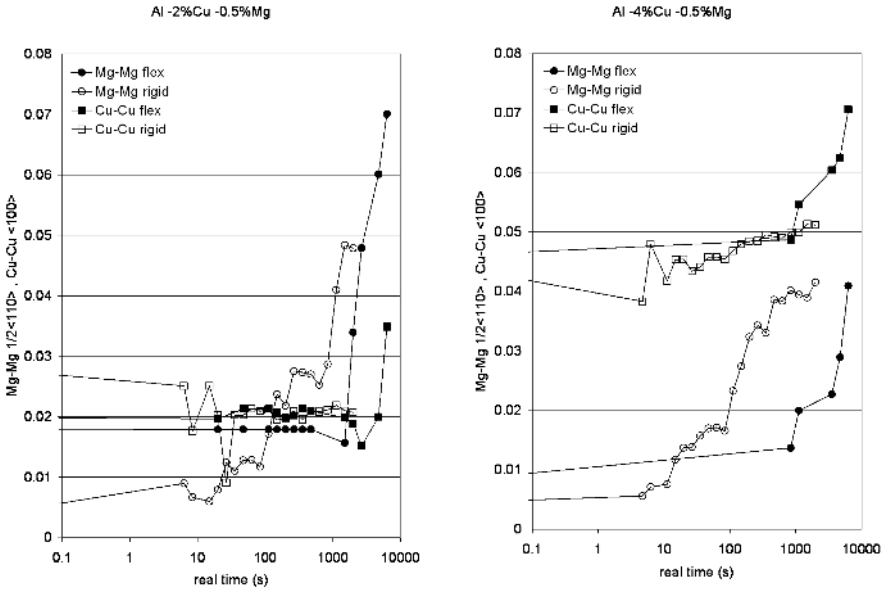

Fig. 5. Ordering in the Al-Cu-0.5%Mg system. These simulations used the same parameters as those in figure 4, and the traces were generated in the same way. Again the magnesium atoms are seen to cluster at later times on a flexible lattice than were seen on the rigid lattice. However, here the clustering of Mg atoms is more extensive, and the clustering of copper atoms reduced

more stable on a flexible lattice than on a rigid lattice. As a result the vacancy mobility may be reduced significantly on a flexible lattice. The exclusion of elastic relaxation in a rigid lattice has the effect of smoothing the configurational potential energy surface, especially in those regions of configuration space where vacancies would have become trapped if elastic interactions had been included.

However, we also saw in figure 3 that the rate of ordering of copper atoms is lower in a rigid lattice than in a flexible lattice. The apparent paradox is resolved by noting that there is a reduced driving force for ordering of copper atoms on a rigid lattice, where bonds are constrained to remain longer than they would be in a relaxed lattice, and this more than outweighs the greater vacancy mobility in a rigid lattice.

A small concentration (0.2 - 0.5 at. %) of magnesium atoms added to the system are rapidly precipitated out of solution in a rigid lattice, owing to the very high energy compressed bonds around each Mg atom. In a flexible lattice the solubility of Mg is enhanced somewhat, and instead their principal action is to reduce severely the vacancy mobility. Mg atoms are especially trapping in a flexible lattice as the compression in the lattice around each atom is alleviated by the formation of a Mg–vacancy pair.

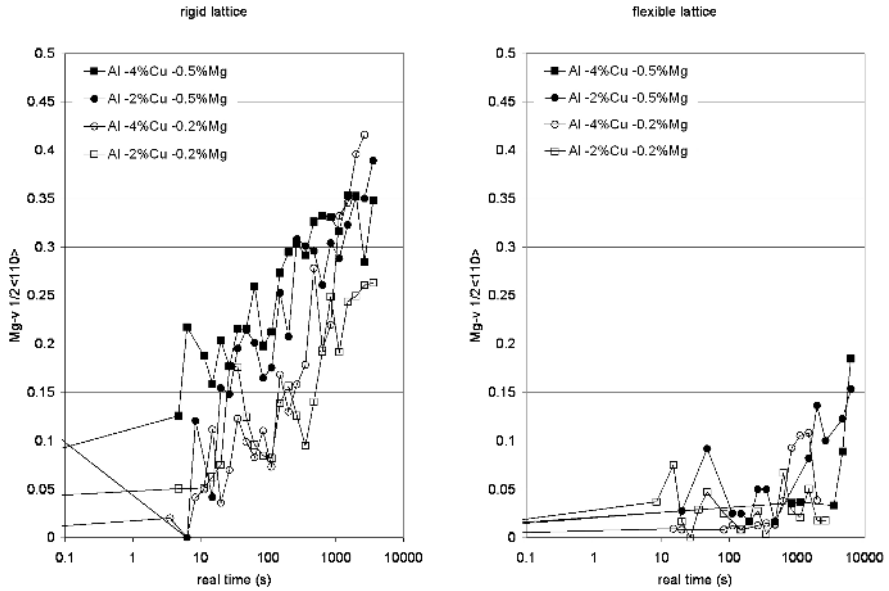

Fig. 6. The proportion of atoms surrounding the vacancy which are magnesium. On a rigid lattice (left) the number of magnesium atoms surrounding a vacancy increases with time. This, together with the clustering of magnesium atoms seen in figs 4 and 5 shows that on a rigid lattice magnesium clusters are forming, and the vacancies are associated with them. On a flexible lattice (right) the number of magnesium atoms around a vacancy is not increasing

5 Acknowledgements

D.R.M was supported by an EPSRC grant. The computer simulations were performed on Oswell, the Oxford University Supercomputer. This work was performed in part under the auspices of the U.S. Department of Energy by the University of California, Lawrence Livermore National Laboratory, under Contract No. W-7405-Eng-48.

References

1. J.T. Veitz and I.J. Polmear. The influence of silver on ageing of Al-Cu-Mg alloys. *J. Inst. Met.*, 94:410—419, 1966.
2. B.C. Muddle and I.J. Polmear. The precipitate Omega phase in Al-Cu-Mg-Ag alloys. *Acta Metall.*, 37(3):777–789, 1989.
3. S.P. Ringer, T. Sakwai, and I.J. Polmear. Origins of hardening in aged Al-Cu-Mg (Ag) alloys. *Acta. Met.*, 45:3731, 1997.
4. H.K. Hardy. The ageing characteristics of some ternary Al-Cu-Mg alloys with Cu:Mg weight ratios of 7:1 and 2.2:1. *J. Inst. Met.*, 84:17–34, 1954.

5. A.K. Mukhopadhyay. Coprecipitation of Omega and sigma phases in Al-Cu-Mg-Mn alloys containing Ag and Si. *Met. Mat. Trans.*, 33A:3635–3648, 2002.
6. K. Hono. Nanoscale microstructral analysis of metallic materials by atom probe field ion microscopy. *Progress in Materials Science*, 47:621–729, 2002.
7. V. Gerold. On the structure of GP zones in Al-Cu alloys. *Scripta Met.*, 22(7):927–932, 1989.
8. J.M. Silcock, T.J. Heal, and H.K. Hardy. Structural aging characteristics of binary aluminium- copper alloys. *J. Inst. Met.*, 82:239, 1954.
9. S.P. Ringer, K. Hono, and T. Sakurai. The effect of trace additions of sn on precipitation in Al-Cu alloys: an atom probe field ion microscopy study. *Met. Mat. Trans. A*, 26A:2207–2217, 1995.
10. J.M. Silcock, T.J. Heal, and H.K. Hardy. The structural ageing characteristics of ternary Al-Cu alloys with Cd,In,Sn. *J. Inst. Met.*, 84:23–32, 1955.
11. J.M. Silcock and H.M. Flower. Comments on a comparison of early and recent work on the effect of trace additions of Cd In or Sn on nucleation and growth of theta prime in Al-Cu alloys. *Scripta Mater*, 46:389–394, 2002.
12. T.T. Rautiainen and A.P. Sutton. Influence of the atomic diffusion mechanism on morphologies, kinetics, and the mechanisms of coarsening during phase separation. *Phys. Rev. B*, 59(21):13681–13692, 1999.
13. R.Weinkamer and P.Fratzl. By which mechanism does coarsening in phase-separating alloys proceed? *Europhys. Lett.*, 61(2):261–267, Jan 2003.
14. D.R. Mason, R.E. Rudd, and A.P. Sutton. Stochastic kinetic Monte Carlo algorithms for long- range Hamiltonians. *Submitted for publication*, 2003.
15. K.A. Fichthorn and W.H. Weinberg. Theoretical foundations of dynamical Monte Carlo simulations. *J. Chem. Phys.*, 95(2):1090–1096, 1991.
16. A.B. Bortz, M.H. Kalos, and J.L. Lebowitz. A new algorithm for Monte Carlo simulation of Ising spin systems. *J. Comp. Phys.*, 17:10–18, 1975.
17. M.A. Novotny. Monte Carlo algorithms with absorbing Markov-chains - fast local algorithms for slow dynamics. *Phys. Rev. Lett.*, 74(1):1–5, 1995.
18. C.P. Flynn. *Point Defects and Diffusion*. Clarendon Press, 1972.
19. M.W. Finnis and J.E. Sinclair. A simple empirical n- body potential for transition metals. *Phil. Mag. A*, 50:45–55, 1984.
20. Y. Saad. *Iterative Methods for Sparse Linear Systems*. PWS, 1996.
21. V. Heine, D.W. Bullett, R. Haydock, and M.J. Kelly. *Solid State Physics*, volume 35. Academic Press, 1980.
22. H. Ikeda and H. Matsuda. Computer simulations of cluster formation processes with relaxation of lattice distortion. *Mater. Trans. JIM*, 33:466–471, 1992.
23. H. Ikeda and H. Matsuda. Effects of difference in elastic moduli between coefficients on spinodal decomposition processes. *Mater. Trans. JIM*, 32:651–657, 1993.
24. H. Ikeda and H. Matsuda. Computer simulation of phase decomposition process generating precipitates harder than matrix. *Mater. Trans. JIM*, 37:1413–1421, 1996.